A Continuously Tunable Microwave Fractional Hilbert Transformer Based on a Nonuniformly Spaced Photonic Microwave Delay-Line Filter

Ze Li, Yichen Han, *Student Member, IEEE*, Hao Chi, Xianmin Zhang, and Jianping Yao, *Fellow, IEEE, OSA*

***Abstract*—A continuously tunable microwave fractional Hilbert transformer (FHT) implemented based on a nonuniformly spaced photonic microwave delay-line filter is proposed and demonstrated. An FHT has a frequency response with a unity magnitude response and a phase response having a phase shift between 0 and π at the center frequency. A seven-tap photonic microwave delay-line filter with nonuniformly spaced taps is designed to provide such a frequency response. The advantage of using nonuniform spacing is that an equivalent negative coefficient can be achieved by introducing an additional time delay leading to a π phase shift, corresponding to a negative coefficient. An FHT operating at a center frequency around 8.165 GHz with a tunable order between 0.24 and 1 is implemented. A classical HT operating at a center frequency of 7.573 GHz with a bandwidth greater than 4.5 GHz is also implemented. The use of the classical HT to perform temporal Hilbert transform of a Gaussian-like electrical pulse is demonstrated.**

***Index Terms*—Chromatic dispersion, fractional Hilbert transform (FHT), optical signal processing, optical single sideband.**

I. Introduction

A MICROWAVE Hilbert transformer (HT), also called a quadrature filter or wideband 90° phase shifter, plays an important role in the theory and practice of microwave signal processing [1], which is widely employed for applications such as communications, radar, and modern instrumentation [1]. To improve the performance of the Hilbert transform and also to permit an additional degree of freedom, the classical HT was generalized to a fractional Hilbert transformer (FHT) [2]. Thus, the classical Hilbert transform can be considered as a special case of the fractional Hilbert transform. In [3] and [4], the discrete version of the fractional Hilbert transform is developed and is applied to achieve single sideband (SSB) modulation, and edge and corner detections of a digital image.

In [5], the implementation of a classical HT based on an integrated electronic delay-line filter was proposed and demonstrated. The major limitation of using pure electronics is the small bandwidth and low operating frequency. Due to the advantages of high speed and broad bandwidth offered by modern optics, the implementation of a microwave HT using photonic techniques has been widely investigated recently [6]–[13]. In [6]–[10], a photonic microwave FHT was implemented based on a phase-shifted uniform fiber Bragg grating (FBG) [6]–[8], a sampled FBG [9], or a Mach–Zehnder interferometer (MZI) [10]. The sampled FBG in [9] and the MZI in [10] were used as a classical HT to implement optical SSB modulation. An FBG-based FHT can perform the transform of an optical pulse with a bandwidth in hundreds of GHz [6]–[8]. The major limitation of an FBG- or MZI-based FHT is that the fractional order is not tunable. In [11] and [12], a classical microwave HT was implemented based on a multitap photonic microwave delay-line filter. The multitap classical HT in [11] was used to achieve two orthogonally phased RF signals, and the HT in [12] was employed to realize instantaneous microwave frequency measurement. However, the implementations of the HT in [11] and [12] were complicated due to the requirement of negative taps and only a classical HT was achieved. In [13], we proposed and demonstrated a continuously tunable microwave FHT based on a multitap photonic microwave delay-line filter using a polarization modulator (PolM). As a PolM was required to achieve the negative tap coefficients in [13], the cost of the system was high and the tuning of the polarization directions of the input light waves was complicated.

Recently, a new concept to achieve a photonic microwave delay-line filter with complex coefficients has been proposed and demonstrated by us, in which the complex coefficients were realized by nonuniform spacing [14]. The use of a nonuniformly spaced photonic microwave delay-line filter for the generation of a phase-coded and a chirped microwave pulse was demonstrated [15], [16]. The use of a nonuniformly spaced photonic microwave delay-line filter to achieve microwave matched filtering was also reported [17]. The key significance of using a nonuniformly spaced delay-line filter to achieve the functionalities is that the filter is easy to implement since the negative or complex coefficients can be equivalently realized through nonuniform spacing.

In this paper, we propose and demonstrate a continuously tunable microwave FHT based on a nonuniformly spaced delay-

Manuscript received October 28, 2011; revised January 27, 2012, March 11, 2012; accepted March 15, 2012. Date of publication March 20, 2012; date of current version April 13, 2012. This work was supported by the Natural Sciences and Engineering Research Council of Canada. The work of Z. Li was supported by a scholarship from the China Scholarship Council.

Z. Li is with the Microwave Photonics Research Laboratory, School of Electrical Engineering and Computer Science, University of Ottawa, Ottawa, ON K1N 6N5, Canada, and also with the Department of Information Science and Electronic Engineering, Zhejiang University, Hangzhou 310027, China.

Y. Han and J. Yao are with the Microwave Photonics Research Laboratory, School of Electrical Engineering and Computer Science, University of Ottawa, Ottawa, ON K1N 6N5, Canada (e-mail: jpyao@eecs.uOttawa.ca).

H. Chi and X. Zhang are with the Department of Information Science and Electronic Engineering, Zhejiang University, Hangzhou 310027, China.

Color versions of one or more of the figures in this paper are available online at http://ieeexplore.ieee.org.

Digital Object Identifier 10.1109/JLT.2012.2191534

line filter. An FHT has a frequency response with a unity magnitude response and a phase response having a phase shift between 0 and π at the center frequency. A continuously tunable FHT with an order tuned at 0.24, 0.52, 0.88, and 1 is implemented based on a seven-tap photonic microwave delay-line filter with nonuniformly spaced taps. The fractional order of the FHT is simply tuned by adjusting the tap coefficient of the central tap. A classical HT operating at a center frequency of 7.573 GHz with a bandwidth greater than 4.5 GHz is also implemented based on an eleven-tap photonic microwave delay-line filter. The use of the classical HT to perform temporal Hilbert transform of a Gaussian-like electrical pulse is demonstrated. The processing error is about 7%. The use of the stopband of the classical HT as a first-order microwave differentiator is discussed.

II. Principle

The ideal frequency response of an FHT can be expressed as [2], [4]

$$H_P(\omega) = \begin{cases} e^{-j\varphi}, & 0 \le \omega < \pi \\ e^{j\varphi}, & -\pi \le \omega < 0 \end{cases} \tag{1}$$

where $\varphi = P \times \pi/2$ denotes the phase and P is the fractional order. As can be seen from (1), an FHT is a φ phase shifter and the FHT becomes a classical HT when $P = 1$. By computing the inverse Fourier transform of $H_P(\omega)$, the corresponding discrete-time impulse response is given by [4]

$$h_P[n] = \begin{cases} \sin(\varphi) \cdot \frac{2}{\pi} \cdot \frac{\sin^2(\pi n/2)}{n}, & n \ne 0 \\ \cos(\varphi), & n = 0. \end{cases} \tag{2}$$

As (2) is the discrete version of the ideal temporal impulse response of the FHT, the corresponding frequency response is periodic and bandwidth limited. Fig. 1(a) shows the normalized $h_P[n]$ for $\varphi = 60°$. As can be seen from (2), the even tap coefficients are all equal to zero except the zeroth and the odd tap coefficients are negative for $n < 0$. Considering that the impulse response of the classical HT is [1]

$$h_1[n] = \begin{cases} \frac{2}{\pi} \cdot \frac{\sin^2(\pi n/2)}{n}, & n \ne 0 \\ 0, & n = 0 \end{cases} \tag{3}$$

thus, by using (3), the impulse response of the FHT can be conveniently rewritten as

$$\begin{aligned} h_P[n] &= \cos(\varphi)\delta[n] + \sin(\varphi)h_1[n] \\ &= \sin(\varphi)\left\{\frac{\cos(\varphi)}{\sin(\varphi)}\delta[n] + h_1[n]\right\} \end{aligned} \tag{4}$$

where $\delta[n]$ is the Dirac delta function. As can be seen from (4), the fractional Hilbert transform of a signal is a weighted sum of the original signal and its classical Hilbert transform [2]. In addition, the order of the FHT is continuously tunable by only adjusting the coefficient of the zeroth tap while keeping the coefficients of the other taps unchanged. However, in this case, the output microwave power is not constant for different fractional orders. The output microwave power for $P = 1$ is about 6 dB lower than that for $P = 1/3$. To solve this problem, in our case, the sum of all the tap coefficients is kept constant and only the ratio between the zeroth tap coefficient and other tap coefficients is adjusted. Then, the variation of the output microwave power is reduced to about 1 dB.

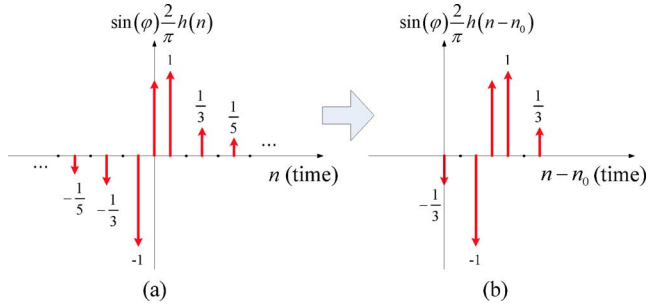

Fig. 1. (a) Ideal time-domain impulse response of the FHT. (b) Delayed and truncated impulse response of the FHT with seven taps.

As the impulse response of the FHT in (2) extends to infinity in time, it should be truncated for practical implementation. In addition, the impulse response exhibits negative time and is anticausal; therefore, for practical implementation, a proper time delay should be introduced to the truncated impulse response to make it a casual system. Thus, the delayed impulse response of the FHT is $h_d[n] = h_P[n - n_0]$, where n_0 is a prescribed delay. The delayed and truncated impulse response of the FHT with seven taps is shown in Fig. 1(b), where $n_0 = 3$. The corresponding frequency response is given by

$$\begin{aligned} H_d(\omega) &= H_P(\omega) \cdot e^{-jn_0\omega} \\ &= \begin{cases} e^{-jn_0\omega}e^{-j\varphi}, & 0 \le \omega < \pi \\ e^{-jn_0\omega}e^{j\varphi}, & -\pi \le \omega < 0. \end{cases} \end{aligned} \tag{5}$$

As can be seen, the time delay will introduce a linear phase to the phase response, but the linear phase has no effect on the output. Usually, an appropriate window function should be applied to the tap coefficients to obtain an optimal tradeoff between the ripples and the bandwidth of the filter. The exact tap coefficients could be obtained by windowing the impulse response after the number of the taps is chosen [11].

According to (2), the frequency response of an FHT based on a delay-line structure can be expressed as [18]

$$\begin{aligned} H_F(\omega) &= \sum_{n=-\infty}^{\infty} h_P[n]e^{-jn\omega T} \\ &= \cos(\varphi) + j\sin(\varphi)\frac{4}{\pi} \\ &\quad \times \left[\sin(\omega T) + \frac{1}{3}\sin(3\omega T) + \cdots\right] \end{aligned} \tag{6}$$

where T is the time delay difference between two adjacent taps. Based on (6), the frequency response of the FHT with different phase shifts (φ) of 20°, 45°, 75°, and 90° is calculated which is shown in Fig. 2, where $T = 125$ ps. Seven taps are used and the free spectral range is 8 GHz. The variations on the phase responses in Fig. 2(a)–(c) are about 5°. The ripples on the magnitude responses are relatively large due to the limited number of taps and the applied rectangular window function in the time domain. To reduce the ripples and increase the 3-dB bandwidth, more taps could be used and the tap coefficients could be adjusted to apply an appropriate window function. To process a baseband signal, the passband of 0–4 GHz is used to perform

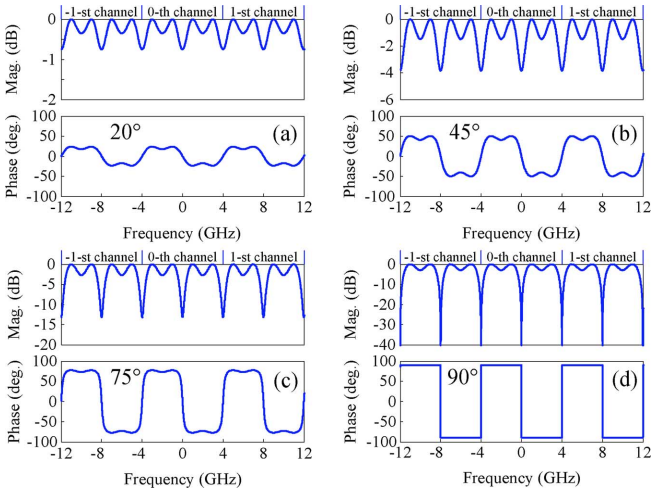

Fig. 2. Frequency responses of the FHT with true negative taps and the phase shifts of 20°, 45°, 75°, and 90°.

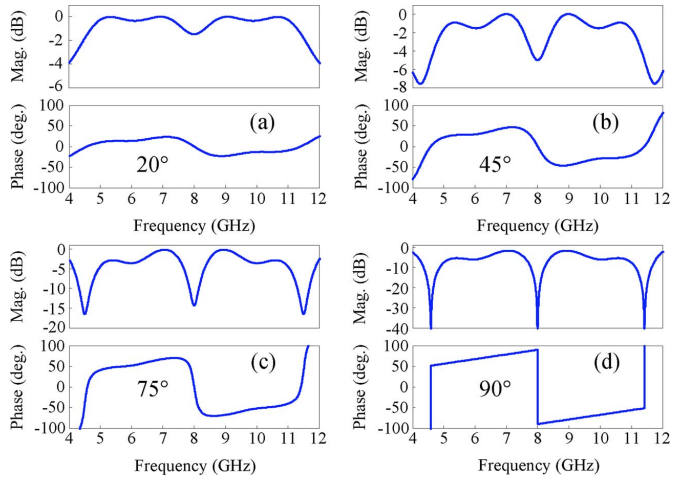

Fig. 3. Frequency responses of the FHT based on nonuniformly spaced microwave delay-line filter with all-positive taps.

the fractional Hilbert transform. However, as shown in Fig. 2, the fractional Hilbert transform could also be performed at 4 or 8 GHz (null point), which makes the filter a bandpass FHT.

As the negative tap coefficients are difficult to achieve in practice, to lower the cost and simplify the implementation, a novel technique to design a filter having equivalent complex coefficients based on a delay-line structure with nonuniform spacing was proposed and demonstrated by us [14], and a comprehensive theoretical study was reported in [19]. According to [14], the time delay and the coefficient of the kth tap in our case at the first channel are given by

$$\tau_k = kT - \frac{\theta[k]}{2\pi}T, \quad a_k = |h_P[k]| \tag{7}$$

where $\theta[n]$ is the phase of $h_P[n]$. For the positive taps, $\theta[k] = 0$ and for the negative taps, $\theta[k] = \pi$. Thus, the frequency response of an FHT based on a nonuniformly spaced delay-line filter can be expressed as

$$\begin{aligned} H_{\mathrm{FN}}(\omega) &= \sum_{k=-\infty}^{\infty} a_k e^{-j\omega\tau_k} \\ &= \cos(\varphi) + \sin(\varphi)\frac{4}{\pi}e^{j\frac{1}{4}\omega T} \\ &\quad \cdot \left[\cos\left(\omega T + \frac{1}{4}\omega T\right)\right. \\ &\quad \left. + \frac{1}{3}\cos\left(3\omega T + \frac{1}{4}\omega T\right) + \cdots\right]. \end{aligned} \tag{8}$$

Fig. 3 shows the frequency response of the FHT with equivalent negative taps at the first channel based on (8). The phase variations are less than 5°. As can be seen from (7) and (8), $H_{\mathrm{FN}}(\omega)$ is exactly equal to $H_F(\omega)$ at the frequency of $\omega = 2\pi/T$; however, a nonlinear phase response is introduced to $H_{\mathrm{FN}}(\omega)$ at other frequencies in the passband when $\varphi \neq 90°$. Fig. 4 shows the phase difference between the phase response of the FHT with true negative taps and that of the FHT with equivalent negative taps. The linear phase difference is eliminated as the linear phase response is equivalent to a pure time delay and has no effect on the output. As can be seen from Fig. 4, an additional

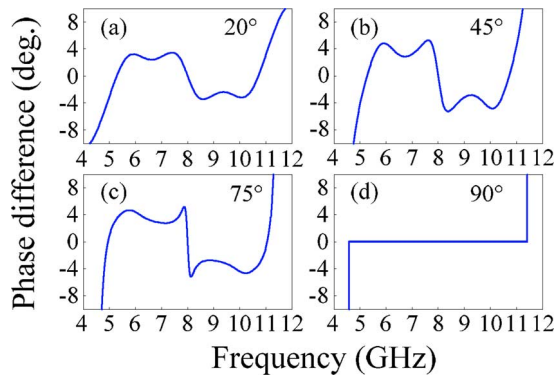

Fig. 4. Phase differences between the phase response of the FHT with true negative taps and that of the FHT with equivalent negative taps.

phase shift of about 3–5° is introduced to the FHT with equivalent negative taps when $\varphi \neq 90°$ and the additional variations introduced to the passband are less than 2°. For practical implementation, a calibration should be performed to adjust the coefficient of the central tap to eliminate the additional phase shift. For example, the theoretical nonzero tap coefficients for 45° phase shift are [0.33, 1, 1.57, 1, 0.33], while the calibrated tap coefficients are [0.33, 1, 1.81, 1, 0.33], which are identical to the theoretical tap coefficients for a phase shift of 41°.

III. Experimental Results

The proposed continuously tunable microwave bandpass FHT based on a seven-tap nonuniformly spaced delay-line filter is then experimentally demonstrated. The experimental setup is shown in Fig. 5. Five wavelengths from five laser diodes (LDs) are multiplexed using an optical coupler and then sent to a Mach–Zehnder modulator (MZM). The optical powers from the LDs are adjusted to ensure that the powers are properly set among the channels, to achieve the required tap coefficients. The intensity-modulated signal is applied to a photodetector (PD) via a length of standard single-mode fiber (SMF). An erbium-doped fiber amplifier (EDFA) is used to compensate the optical power loss and keep the optical power incident on the PD constant, which also makes the sum of all

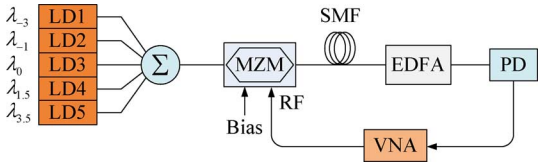

Fig. 5. Experimental setup for the FHT based on a nonuniformly spaced photonic microwave delay-line filter.

the tap coefficients constant. Due to the dispersion of the SMF, a time delay difference between two wavelengths is generated. The length of the SMF is about 24.7 km, and the chromatic dispersion is calculated to be $\chi = 407.6$ ps/nm when the wavelength is around 1545 nm. Since the time delay difference between two taps is proportional to the wavelength spacing, the optical wavelength of the kth tap is calculated by [14]

$$\lambda_k = \frac{\tau_k - \tau_{-3}}{\chi} + \lambda_{-3} \tag{9}$$

where λ_{-3} and λ_k are the wavelengths of the first and the kth nonzero taps. In the experiment, the wavelengths of the LDs are tuned to achieve the required nonuniformly spaced time delay differences based on (9). The power of each LD is also adjusted to obtain the desired tap coefficients. By tuning the coefficient (laser power) of the zeroth tap (λ_0) while keeping the coefficients of the other taps unchanged, a continuously tunable bandpass FHT is achieved. Fig. 6 shows the frequency response of the FHT with different unrecovered phase shifts (φ) of 18°, 42°, 75°, and 90°. The wavelengths of the nonzero taps are set at [1543.680, 1544.280, 1544.730, 1545.030, 1545.630] nm, which makes the center frequency of the FHT at about 8.165 GHz. The phase shifts in Fig. 6(a) and (b) were originally designed to be 20° and 45°; however, an about 2° error was introduced during the power-tuning process of LD3. Small errors also exist on other phase responses, but the experimental results still agree very well with the theoretical results. Fig. 7 shows the recovered phase response from Fig. 6 with the linear phase eliminated. As can be seen, an additional phase shift of about 4° is introduced when $\varphi \neq 90°$, and the phase variations are all within ±5° in the passband, which shows excellent agreement with the previous prediction.

To increase the 3-dB bandwidth and reduce the variations on the magnitude response, another classical HT with eleven taps is designed. In the design, the wavelengths of the nonzero taps are set at [1543.190, 1543.790, 1544.390, 1545.140, 1545.740, 1546.340] nm and the length of the SMF is adjusted to be 22.8 km, which makes the center frequency of the HT at about 8.86 GHz, and the tap coefficients are set to be [0.09, 0.23, 1, 1, 0.23, 0.09]. The frequency response of the bandpass HT is shown in Fig. 8(a), which is measured using a vector network analyzer (VNA, Agilent E8364A), as shown in Fig. 5. As can be seen, the center frequency is 8.857 GHz and the phase shift is close to π. The operating bandwidth is about 5.4 GHz and the ripples of the phase within the passband are less than 3°. Then, to demonstrate the frequency tunability, we tune the wavelengths at [1542.890, 1543.590, 1544.290, 1545.165, 1545.865, 1546.565] nm and the tap coefficients are set to be [0.13, 0.22, 1, 1, 0.22, 0.13]. The frequency response of the classical HT is shown in Fig. 8(b). It

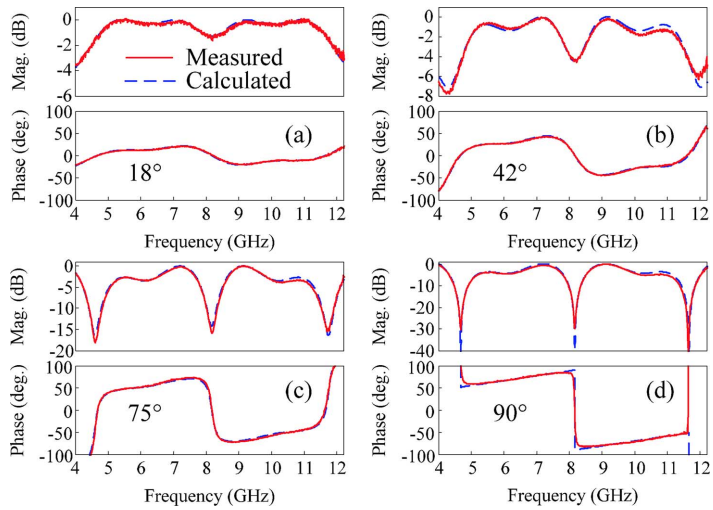

Fig. 6. Measured and calculated frequency responses of the FHT with equivalent negative taps and unrecovered phase.

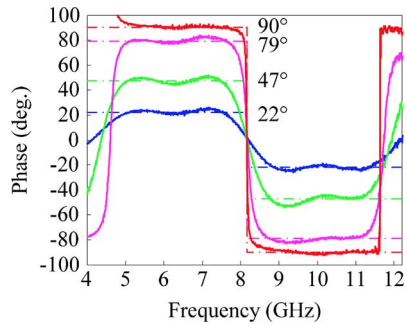

Fig. 7. Recovered phase response of the FHT with the linear phase eliminated.

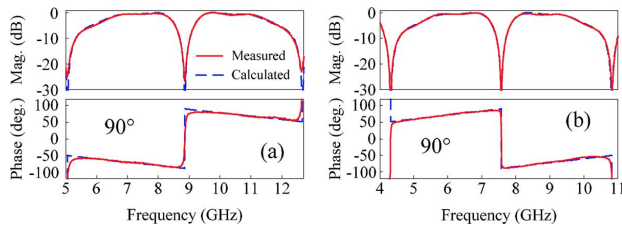

Fig. 8. Measured and calculated frequency responses of a classical HT with equivalent negative taps and different center frequencies. (a) 8.857 GHz. (b) 7.573 GHz.

can be seen that the center frequency is now 7.573 GHz and the bandwidth is about 4.6 GHz. The phase shift agrees very well with the theoretical prediction. The ripples of the linear phase in the passband are also within ±3°.

To verify that the proposed nonuniformly spaced microwave delay-line filter can be used to implement real-time temporal Hilbert transform, an electrical pulse from an arbitrary waveform generator (AWG, Tektronix AWG7102), shown in Fig. 9(a), is mixed with a 7.573-GHz signal from a local oscillator (LO) at an electrical mixer and applied to the MZM. The pulse from the AWG has a shape close to Gaussian with a full-width at half-maximum of about 0.47 ns and a bandwidth of about 2.3 GHz. The electrical pulse output from the PD is downconverted to the baseband at another electrical mixer with the same LO. The output waveform is observed by a digital

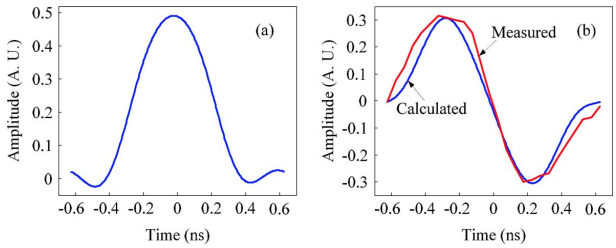

Fig. 9. Experimental results. (a) Input pulse from the AWG. (b) Theoretically calculated and the experimentally measured Hilbert-transformed pulses.

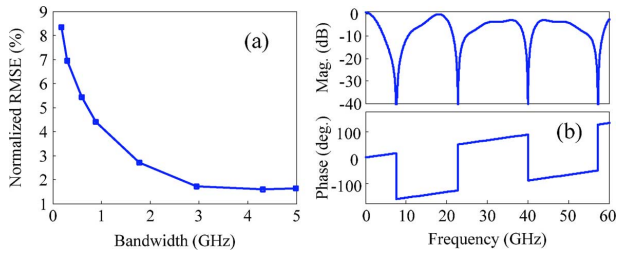

Fig. 10. (a) Simulated processing error as a function of the input pulse bandwidth for the classical HT shown in Fig. 8(b). RMSE: root mean square error. (b) Frequency response of a classical HT with equivalent negative taps and the center frequency of 40 GHz.

phosphor oscilloscope (Tektronix TDS7704B). Fig. 9(b) shows the theoretically calculated and the experimentally measured Hilbert-transformed pulses. As can be seen, the calculated and measured pulses agree well. The root mean square error (RMSE) is calculated to be 7.16%, which is normalized to the peak-to-peak value of the calculated Hilbert-transformed output pulse.

IV. Discussion and Conclusion

The processing error as a function of the input pulse bandwidth is calculated based on the measured magnitude and phase responses of the bandpass classical HT shown in Fig. 8(b). The input is an ideal Gaussian pulse with different bandwidths. The processing error is then obtained by calculating the normalized RMSE between the calculated output pulse using the measured classical microwave HT and the theoretical Hilbert transform of the input ideal Gaussian pulse, as shown in Fig. 10(a). It can be seen that the processing error is larger when the bandwidth of the input pulse is smaller due to the notch at the center frequency of the magnitude response.

As can be seen from Figs. 2 and 3, the bandwidth of the proposed FHT with equivalent negative taps is smaller than the original FHT with true negative taps. This is due to the narrow-bandwidth feature of the nonuniformly spaced delay-line filter [14]. The bandwidth of the proposed FHT could be increased by increasing the center frequency. Fig. 10(b) shows the frequency response of a classical HT based on an eleven-tap nonuniformly spaced filter. The center frequency is 40 GHz. As can be seen, the bandwidth of the HT is increased to about 24 GHz, which is much larger than those in Fig. 3. For broader bandwidth operation, the power fading effect resulted from the chromatic dispersion of the dispersive fiber should also be taken into consideration [20].

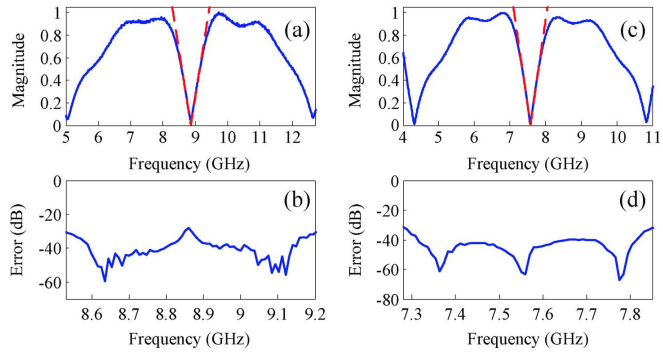

Fig. 11. (a) Magnitude responses of the HT shown in Fig. 8(a) and the corresponding ideal differentiator. (b) Error between the HT and the ideal differentiator in (a). (c) Magnitude responses of the HT shown in Fig. 8(b) and the corresponding ideal differentiator. (d) The error between the HT and the ideal differentiator in (c).

It was shown in [21] that a first-order optical HT could also function as a first-order temporal optical differentiator in the stopband. This also applies to the microwave bandpass HT in our case, which also functions as a first-order microwave differentiator. Fig. 11 shows the magnitude responses of the classical HT shown in Fig. 8 and the corresponding ideal differentiator. The operating bandwidths are 0.66 and 0.56 GHz, respectively, in Fig. 11(a) and (b). As can be seen, the experimental result agrees very well with the ideal result and the error is smaller than -30 dB in the entire passband of the differentiator.

In conclusion, we have proposed and demonstrated a continuously tunable bandpass FHT based on a nonuniformly spaced delay-line filter. An FHT with a tunable order at 0.24, 0.52, 0.88, and 1 and a center frequency of 8.165 GHz was implemented. A classical HT operating at a center frequency of 7.573 GHz with a bandwidth greater than 4.5 GHz was also implemented based on an eleven-tap nonuniformly spaced microwave delay-line filter. The use of the classical HT to perform temporal Hilbert transform of a Gaussian-like electrical pulse was demonstrated. The processing error as a function of the input pulse bandwidth was estimated based on the frequency response of the measured classical microwave HT. The use of the stopband of the classical HT as a first-order microwave differentiator was also discussed.

References

[1] S. L. Hahn, , A. D. Poularikas, Ed., *Transforms and Applications Handbook*, 3rd ed. Boca Raton, FL: CRC Press, 2010, ch. 7.
[2] A. W. Lohmann, D. Mendlovic, and Z. Zalevsky, "Fractional Hilbert transform," *Opt. Lett.*, vol. 21, no. 4, pp. 281–283, Feb. 1996.
[3] S. C. Pei and M. H. Yeh, "Discrete fractional Hilbert transform," *IEEE Trans. Circuits Syst. II, Analog Digital Signal Process.*, vol. 47, no. 11, pp. 1307–1311, Nov. 2000.
[4] C. C. Tseng and S. C. Pei, "Design and application of discrete-time fractional Hilbert transformer," *IEEE Trans. Circuits Syst. II, Analog Digital Signal Process.*, vol. 47, no. 12, pp. 1529–1533, Dec. 2000.
[5] C. D. Holdenried, J. W. Haslett, and B. Davies, "A fully integrated 10-Gb/s tapped delay Hilbert transformer for optical single sideband," *IEEE Microwav. Wireless Compon. Lett.*, vol. 15, no. 5, pp. 303–305, May 2005.
[6] M. H. Asghari and J. Azaña, "All-optical Hilbert transformer based on a single phase-shifted fiber Bragg grating: Design and analysis," *Opt. Lett.*, vol. 34, no. 3, pp. 334–336, Feb. 2009.
[7] M. Li and J. P. Yao, "All-fiber temporal photonic fractional Hilbert transformer based on a directly designed fiber Bragg grating," *Opt. Lett.*, vol. 35, no. 2, pp. 223–225, Jan. 2010.

[8] M. Li and J. P. Yao, "Experimental demonstration of a wideband photonic temporal Hilbert transformer based on a single fiber Bragg grating," *IEEE Photon. Technol. Lett.*, vol. 22, no. 21, pp. 1559–1561, Nov. 2010.
[9] X. Y. Wang, M. Hanawa, K. Nakamura, K. Takano, and K. Nakagawa, "Sideband suppression characteristics of optical SSB generation filter with sampled FBG based 4-taps optical Hilbert transformer," in *Proc. Asia Pacific Conf. Commun.*, 2009, pp. 622–625.
[10] K. Takano, N. Hanzawa, S. Tanji, and K. Nakagawa, "Experimental demonstration of optically phase-shifted SSB modulation with fiber-based optical Hilbert transformers," presented at the Tech. Digest Opt. Fiber Commun. Conf./Nat. Fiber Opt. Eng. Conf., Anaheim, CA, 2007, Paper JThA48.
[11] H. Emami, N. Sarkhosh, L. A. Bui, and A. Mitchell, "Wideband RF photonic in-phase and quadrature-phase generation," *Opt. Lett.*, vol. 33, no. 2, pp. 98–100, Jan. 2008.
[12] H. Emami, N. Sarkhosh, L. A. Bui, and A. Mitchell, "Amplitude independent RF instantaneous frequency measurement system using photonic Hilbert transform," *Opt. Exp.*, vol. 16, no. 18, pp. 13707–13712, Sep. 2008.
[13] Z. Li, W. Li, H. Chi, X. Zhang, and J. P. Yao, "A continuously tunable microwave fractional Hilbert transformer based on a photonic microwave delay-line filter using a polarization modulator," *IEEE Photon. Technol. Lett.*, vol. 23, no. 22, pp. 1694–1699, Nov. 2011.
[14] Y. Dai and J. P. Yao, "Nonuniformly-spaced photonic microwave delay-line filter," *Opt. Exp.*, vol. 16, no. 7, pp. 4713–4718, Mar. 2008.
[15] Y. Dai and J. P. Yao, "Microwave pulse phase encoding using a photonic microwave delay-line filter," *Opt. Lett.*, vol. 32, no. 24, pp. 3486–3488, Dec. 2007.
[16] Y. Dai and J. P. Yao, "Chirped microwave pulse generation using a photonic microwave delay-line filter with a quadratic phase response," *IEEE Photon. Technol. Lett.*, vol. 21, no. 9, pp. 569–571, May 2009.
[17] Y. Dai and J. P. Yao, "Microwave correlator based on a nonuniformly spaced photonic microwave delay-line filter," *IEEE Photon. Technol. Lett.*, vol. 21, no. 14, pp. 969–971, Jul. 2009.
[18] J. Capmany, B. Ortega, and D. Pastor, "A tutorial on microwave photonic filters," *J. Lightw. Technol.*, vol. 24, no. 1, pp. 201–229, Jan. 2006.
[19] Y. Dai and J. P. Yao, "Nonuniformly spaced photonic microwave delay-line filters and applications," *IEEE Trans. Microw. Theory Tech.*, vol. 58, no. 11, pp. 3279–3289, Nov. 2010.
[20] Y. Park, M. Asghari, R. Helsten, and J. Azana, "Implementation of broadband microwave arbitrary-order time differential operators using a reconfigurable incoherent photonic processor," *IEEE Photon. J.*, vol. 2, no. 6, pp. 1040–1050, Dec. 2010.
[21] N. Q. Ngo and Y. Song, "On the interrelations between an optical differentiator and an optical Hilbert transformer," *Opt. Lett.*, vol. 36, no. 6, pp. 915–917, Mar. 2011.

Ze Li received the B.S. degree in electrical engineering from Zhejiang University, Hangzhou, China, in 2007. He is currently working toward the Ph.D. degree as a joint training student in the Department of Information and Electronic Engineering, Zhejiang University, and the School of Electrical Engineering and Computer Science, University of Ottawa, Ottawa, ON, Canada.

His current interests include microwave photonics, optical pulse processing, fiber-Bragg-grating-based devices, and optical communications.

Yichen Han (S'10) received the B.Eng. degree in telecommunication engineering from the Beijing University of Posts and Telecommunications, Beijing, China, in 2009. He is currently working toward the M.A.Sc. degree in electrical and computer engineering in the School of Electrical Engineering and Computer Science, University of Ottawa, Ottawa, ON, Canada.

His research interests include optical microwave signal processing and pulse shaping.

Hao Chi, biography not available at the time of publication.

Xianmin Zhang, biography not available at the time of publication.

Jianping Yao (M'99–SM'01–F'12) received the Ph.D. degree in electrical engineering from the Université de Toulon, Toulon, France, in December 1997.

He joined the School of Electrical Engineering and Computer Science, University of Ottawa, Ottawa, ON, Canada, as an Assistant Professor, in 2001, where he became an Associate Professor in 2003 and Full Professor in 2006. He was appointed University Research Chair in 2007. He was the Director of the Ottawa-Carleton Institute for Electrical and Computer Engineering from July 2007 to June 2010. Prior to joining the University of Ottawa, he was an Assistant Professor in the School of Electrical and Electronic Engineering, Nanyang Technological University, Singapore, from 1999 to 2011. His research has focused on microwave photonics, which includes photonic processing of microwave signals, photonic generation of microwave, mm-wave and THz, radio over fiber, ultrawideband over fiber, and photonic generation of microwave arbitrary waveforms. His research also covers fiber optics and biophotonics, which includes fiber lasers, fiber and waveguide Bragg gratings, fiber-optic sensors, microfluidics, optical coherence tomography, and Fourier-transform spectroscopy. He is a principal investigator of over 20 projects, including five strategic grant projects funded by the Natural Sciences and Engineering Research Council of Canada. He has contributed to more than 360 papers, including more than 200 papers in peer-reviewed journals and 160 papers in conference proceedings.

Dr. Yao is a registered Professional Engineer of Ontario. He is a Fellow of the Optical Society of America, and a Fellow of the IEEE Microwave Theory and Techniques Society and the IEEE Photonics Society. He is an Associate Editor of the *International Journal of Microwave and Optical Technology*. He is on the Editorial Board of the IEEE TRANSACTIONS ON MICROWAVE THEORY AND TECHNIQUES. He is a Chair of numerous international conferences, symposia, and workshops, including Vice TPC Chair of 2007 IEEE Microwave Photonics Conference, TPC Co-Chair of 2009 and 2010 Asia-Pacific Microwave Photonics Conference, TPC Chair of the high-speed and broadband wireless technologies sub-committee of 2009, 2010, 2011, and 2012 IEEE Radio Wireless Symposium, TPC Chair of the microwave photonics sub-committee of 2009 IEEE Photonics Society Annual Meeting, TPC Chair of 2010 IEEE Microwave Photonics Conference, and General Co-Chair of 2011 IEEE Microwave Photonics Conference. He is also a committee member of numerous international conferences. He received the 2005 International Creative Research Award of the University of Ottawa. He was the recipient of the 2007 George S. Glinski Award for Excellence in Research. He was a recipient of a Natural Sciences and Engineering Research Council of Canada Discovery Accelerator Supplements Award in 2008.